Hydrol. Earth Syst. Sci., 15, 2091–2099, 2011
www.hydrol-earth-syst-sci.net/15/2091/2011/
doi:10.5194/hess-15-2091-2011

Hydrology and Earth System Sciences

Drainage basin morphometry: a global snapshot from the shuttle radar topography mission

P. L. Guth

Department of Oceanography, US Naval Academy, Annapolis, MD, USA

Received: 3 January 2011 – Published in Hydrol. Earth Syst. Sci. Discuss.: 16 February 2011
Revised: 3 June 2011 – Accepted: 21 June 2011 – Published: 7 July 2011

Abstract. A suite of 42 morphometric parameters for each of 26 272 drainage basins larger than 100 km^2 from the Hydrosheds Shuttle Radar Topography digital elevation model shows the global distribution of Strahler order for streams and drainage basins. At the scale of 15 arc s spacing (232 to 464 m) the largest basins are order 9. Many common parameters depend both on the size of the basin, and the scale of the digital elevation model used for the computations. These drainage basins display the typical longitudinal stream profiles, but the major basins tend to be generally more concave than the smaller basins.

1 Introduction

The Shuttle Radar Topography Mission (SRTM) created a near global digital elevation model (DEM) with 3 arc s spacing, about 90 m (Farr et al., 2007). Despite some voids in mountainous terrain and sandy desert regions, the SRTM DEM remains the best freely available dataset and several projects have worked to fill the voids (Jarvis et al., 2008; Lehner et al., 2008a,b). The SRTM's greatest weakness is the lack of coverage for Antarctica and latitudes north of 60°, so the north-flowing rivers in North America and Eurasia are under-represented, either missing or truncated at the limits of SRTM coverage.

The Hydrosheds project (Lehner et al., 2008a,b) created a hole-filled version of the SRTM DEM, conditioned the dataset for hydrologic applications, and released a drainage network and basin outlines from a 15 arc s version of SRTM. This data set includes 3.46 million stream segments in 2.48 million basins; most of the basins are small and contain at most one stream segment. A segment connects two nodes, with a node being either the terminus of a segment or the junction of two segments. The largest 1.06 % of the basins, those over 100 km^2 in area, contain 98.64 % of the stream segments.

Geomorphometry performs quantitative land-surface analysis (Pike et al., 2009), and the SRTM data provides a data set at an appropriate scale for global analyses. Guth (2006) looked at 12 key morphometric parameters from SRTM to compare results with the US National Elevation Dataset, and further described 30 parameters computed worldwide from SRTM (Guth, 2009). Those analyses used small rectangular areas 2.5 arc min on a side (0.5 million areas in the United States, 7.4 million in the entire world) which can be considered random sampling areas.

This study uses the Hydrosheds drainage basins (Lehner et al., 2008a,b), natural sampling areas of varying size, and computes both morphometric parameters from the DEM, metrics of the drainage basin and channel networks, and characteristics of the channel thalwegs.

2 Methods and limitations

Appendix A lists the processing steps used with the Hydrosheds data. I excluded basins with an area less than 100 km^2. With the 15″ DEM used to compute the drainage network, each pixel is about 464x461 m at the equator and 232×464 m at 60°, the limit of the SRTM data. These represent about 0.2 km^2 and 0.1 km^2 respectively, so a 100 km^2 drainage basin contains 500–1000 elevation points. These basins are likely to have only a single recognizable channel, and produce statistics of limited validity. While this size limit is somewhat arbitrary, over 85 % of the drainage basins identified by Hydrosheds have areas less than 1 km^2 and most of these have no channel segments. Most of these small basins occur on the coastline, or large areas of interior drainage (Fig. 1).

Correspondence to: P. L. Guth
(pguth@usna.edu)

Published by Copernicus Publications on behalf of the European Geosciences Union.

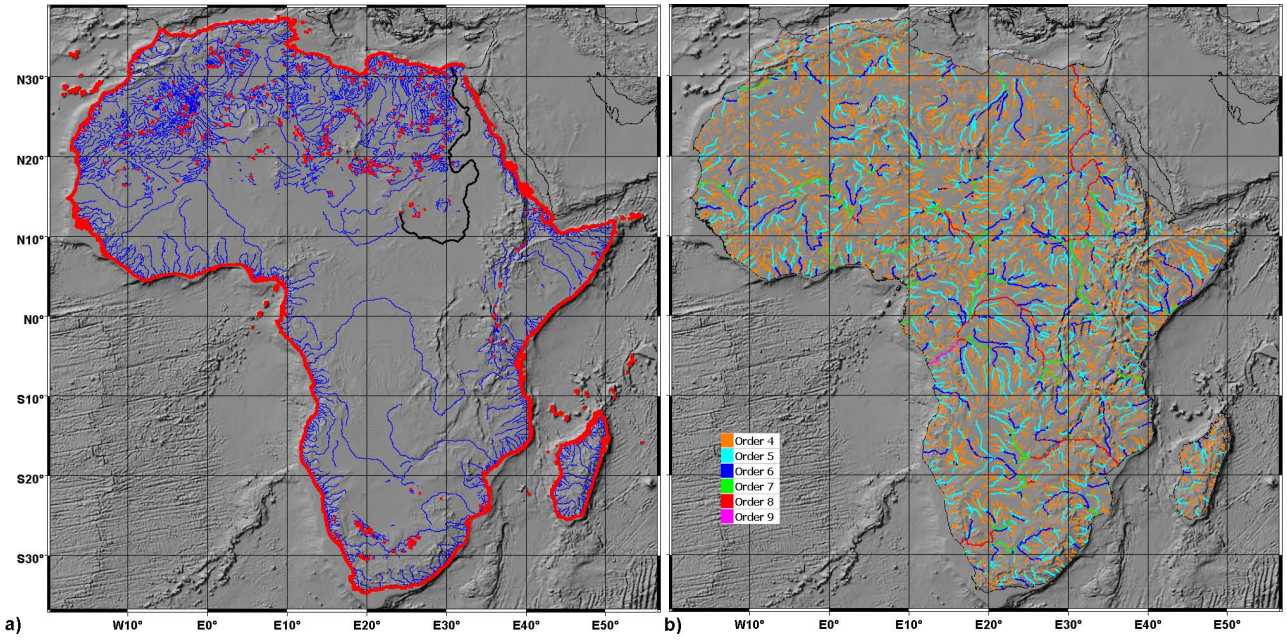

Fig. 1. (a) Red symbols mark drainage basins smaller than 100 km^2 for Africa, with the thalwegs of the larger drainage basins shown in blue. The Nile is highlighted in black. The small basins effectively mark the coastline, with smaller numbers in interior drainage areas such as the Sahara. The size of the symbols greatly exaggerates the importance of the small basins. **(b)** Strahler order for the larger channels in Africa, down to order 4.

The scale of the DEM used to create the drainage network limits the scale of features visible in the drainage networks. The smallest segments will be a single pixel, about a half kilometer, and will influence parameters like sinuosity, so care must be taken in comparing these results with those from different scales.

Computed thalwegs (the major channel in the basin) are based solely on landforms in the SRTM data, and not on hydrology; some channels might be intermittent or almost always dry. The thalwegs start from the last river segment in the basin, which has the largest contributing area and no downstream connections. I trace the thalweg upstream, at each junction taking the tributary with the larger contributing area. This algorithm can be fooled in cases where climate does not produce rainfall and runoff proportional to area; the Nile, highlighted in Fig. 1, shows the computed thalweg following the Bahr el Ghazal and Bahr al-Arab (tributaries of the White Nile) west into Darfur, instead of following the water up the Blue Nile. The number of basins in the data set precludes a manual search to correct this limitation.

Figure 2 compares the Hydrosheds drainage network with the medium resolution network from the US National Hydrography Dataset (NHD; Simley and Carswell, 2009). At regional scales they line up very well, and because the NHD reflects a larger scale, it generally shows additional tributaries. The number of additional tributaries varies with landforms and the resulting channel patterns. Brief qualitative assessment suggests that the Strahler order 1 streams in this

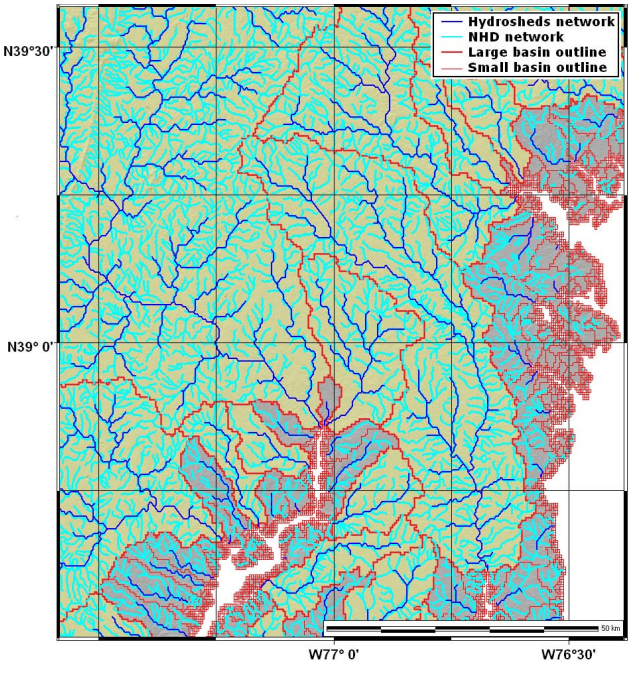

Fig. 2. Comparison of Hydrosheds and NHD drainage networks for part of the Chesapeake Bay watershed.

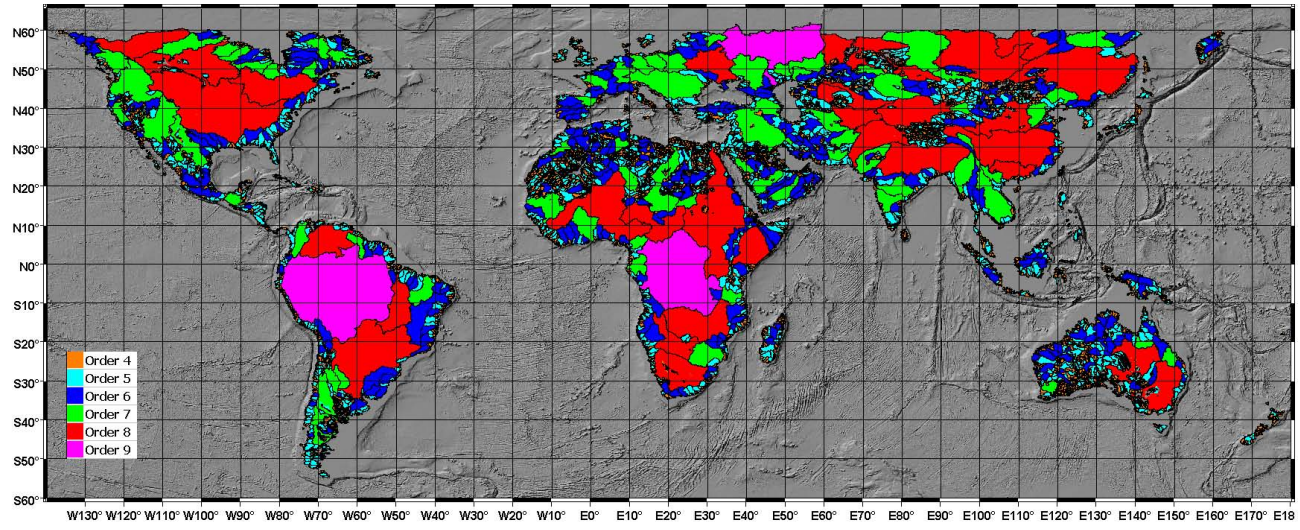

Fig. 3. Strahler order for the largest segment in global drainage basins.

region range from order 1 to 4 in the NHD data, and most commonly are order 2 or 3. Figure 2 also shows the bimodal distribution of the areas for small basins ($<100\,km^2$): a great many tiny basins along the coast with no stream segments, and a much smaller number of first and some second order drainage networks between the outlets of the larger basins.

3 Results

Figure 3 shows the drainage basins coded by Strahler order. Three rivers (Amazon, Congo, and Volga) have the largest Strahler order of 9, and very different geomorphic regimes due to significant differences in total basin relief (6211, 3955, and 1624 m respectively). The maps on Fig. 3, and those later on Fig. 5, visually emphasize the large basins, and several key characteristics stand out. The desert belts (North American Great Basin, Sahara, Arabian peninsula, central Asia, and western Australia) lack large drainage basins, in both area and Strahler order. Figure 4a shows a histogram of Strahler order for the 26 272 basins with an area greater than $100\,km^2$, clearly demonstrating a logarithmic decline in the number of basins with increasing order, and a truncation in the distribution for at least order 1 streams. Figure 4b shows the number of basins versus basin area, and Fig. 4c shows basin area versus Strahler order, with both diagrams showing the truncation of the data set at $100\,km^2$ basin area. Limiting basin size to $100\,km^2$ removes many small order 1 streams; an alternative might be to restrict analysis to higher order streams. Figure 4a and c suggests that order 4 and higher basins might be most appropriate for this data set, and not suffer artificial truncation other than the coverage limits of the SRTM for the Arctic rivers.

Figure 5 shows maps color-coded by some of the basin morphometric parameters listed in Appendix B. ELEV_RELF (Fig. 5a) is the elevation-relief ratio computed from the DEM. The Dnieper River basin has the largest value of this parameter for a major basin, due to an elevation distribution with almost all the points in the middle of the elevation distribution and very little area near the elevation of the Black Sea, and a thalweg which descends comparatively rapidly near its mouth at the Black Sea. Figure 5b shows the RATIO_RELF parameter, which considers only the geometry of the thalweg and in essence computes its average slope. The largest values occur in small steep basins which do not show up well at this scale; of major rivers, the largest RATIO_RELF values are from the Mekong and Yangtze, which have thalwegs that rapidly ascend high into the central Asian mountains. Figure 5c shows the log of BASIN_RUGD, the ratio of basin's elevation range to its area, and this metric rewards small, steep basins along coasts and interior basins in central Asia; coloring by the logarithm emphasizes the huge range and uneven distribution in values for this parameter, from nearly 0 for the many very large, flat basins to 36 for a relatively few small steep basins. Figure 5d shows thalweg SINUOSITY, with low values for a straight thalweg and higher values for curved channels. The most sinuous major river that appears at this scale is the Don, which curves 1896 km to travel a straight line distance of 521 km. Figure 5e shows the percentage of the basin area with slopes steeper than 30 %, which correspond with the major mountain belts and some steep coastal highlands like those bordering the Red Sea. Figure 5f shows the relief of the main thalweg, and highlights the major rivers that drain the Andes and the mountains of central Asia.

Figures 6 and 7 look at main thalwegs, on a normalized plot of elevation and distance so that profile shapes can be

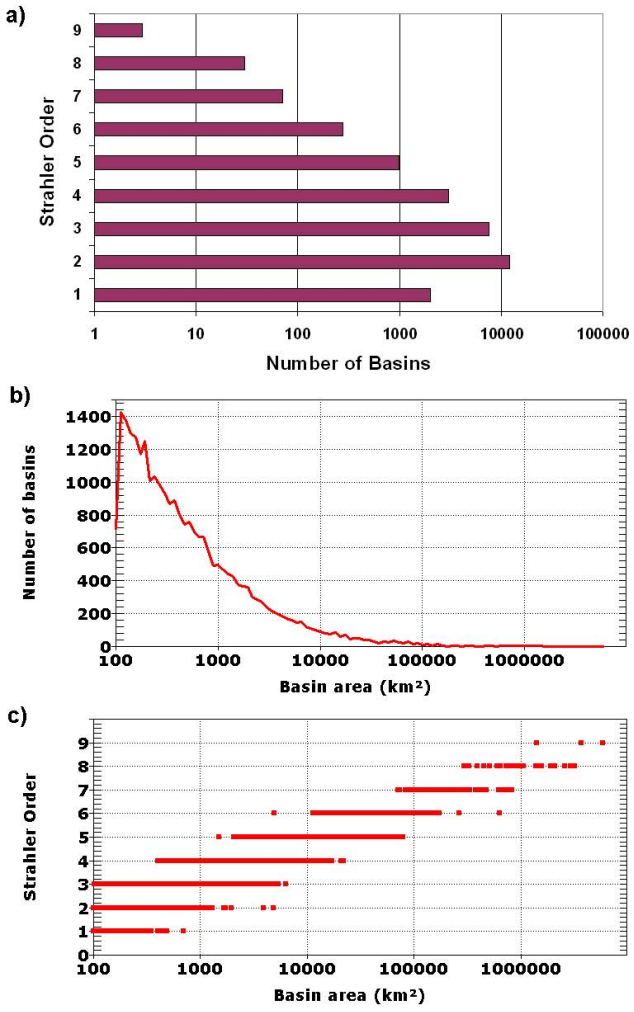

Fig. 4. (a) Histogram of Strahler order. **(b)** Histogram of basin area. **(c)** Basin area versus Strahler order.

compared despite different lengths and elevation differences. Figure 6 contours the density of thalweg shapes. The normalized profiles are broken into 100 intervals horizontally and vertically, and the number of profiles that pass through each interval tallied. The contoured plots shows the density of the profiles going through each percentage interval on the graph. The blue represents a value greater than or equal to 1, and the magenta includes values significantly larger than 5 near the two ends of the graph where normalization forces the profiles through (0, 0) and (100, 100). Profiles tend to be very gentle near the mouth of the river, and steep near the headwaters, reflecting the traditional graded profile. The small basins, which dominate Fig. 6a, tend to have a much more linear profile; the larger streams tend to have a flatter downstream segment, steeper headwaters, and an overall more concave profile as seen in Fig. 6b. Figure 7 shows the thalwegs of the 25 largest basins (defined as having over 500 m relief along the thalweg, and Strahler order 8 or 9). We have filtered

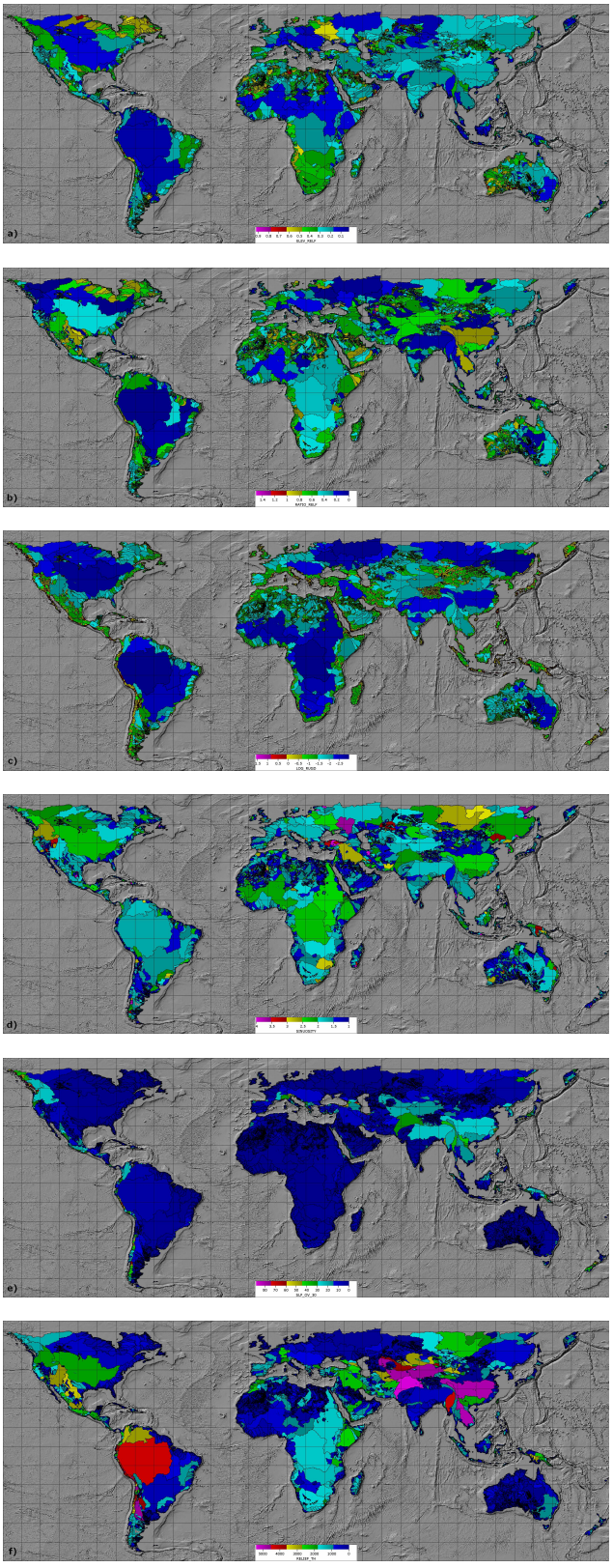

Fig. 5. Maps with drainage basin parameters. **(a)** ELEV_RELF, **(b)** RATIO_RELF, **(c)** LOG_RUGD, **(d)** SINUOSITY, **(e)** percentage of basin with slopes over 30 %, and **(f)** relief of the main thalweg.

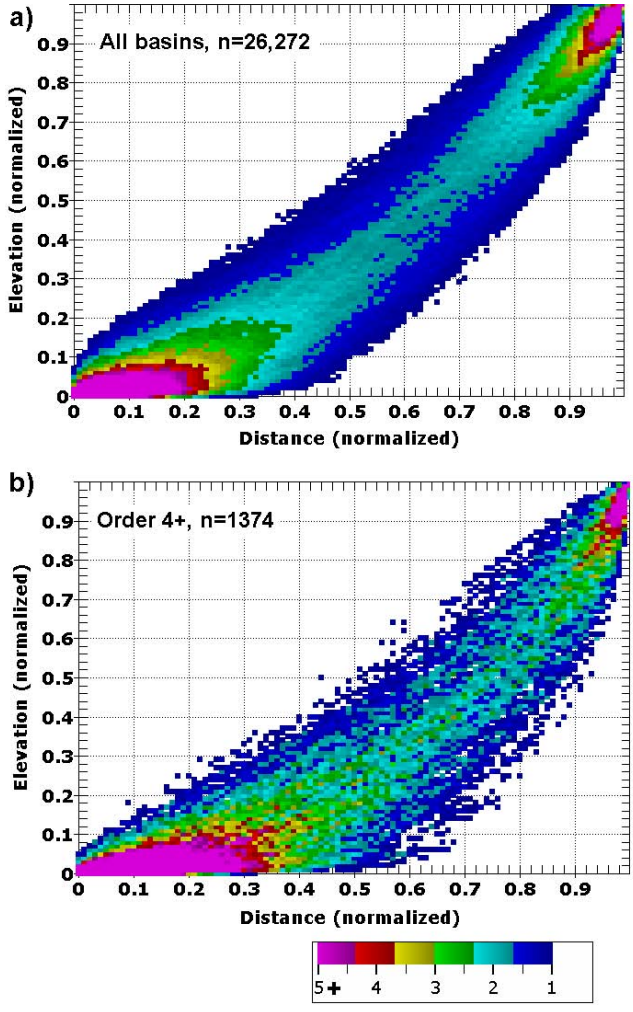

Fig. 6. Density of normalized longitudinal thalweg profiles for all basins **(a)** and those of Strahler order 4 and larger **(b)**. The density records the percentage of thalwegs in percentile bins both horizontally and vertically. Colors range from 1 % (blue) to 5 % or greater (violet). Note the displacement downward and to the right for the larger basins.

the profiles for downstream decrease in elevation, as the 3-D shapfiles contain anomalous noise for some rivers as an artefact of the hydrological conditioning. A number of the thalwegs in Fig. 7 lie outside the common zones seen in Fig. 6; for example, both the Amazon and Niger (Fig. 7b) have extremely steep headwaters, while the Nelson has an extremely abrupt descent into Hudson Bay, as well as much lower overall relief compared to the others in this group. Several of these thalwegs, such as the Indus and Zambezi, show several distinct convex segments.

Figure 8 shows a correlation matrix for the 42 parameters in Appendix B, for all 26 272 basins. Blue represents the strength of positive correlations, and red negative correlations. Parameters are organized by their average correlation (r^2) with the other 41 parameters. Positive correlations > 0.90 in the upper left corner of the diagram mostly demonstrate that many of the parameters really reflect different ways of expressing slope, including the inverse slope measures such as S1S2 and STRENGTH. The strongest correlations not directly related to slope include the log of the basin area, the Strahler order, length of the main basin thalweg, and the basin perimeter, which all measure the basin size.

Parameters at the bottom of Fig. 8 fall into two categories. Some, such as S2S3 and SHAPE, do not reveal much information at the scale of large drainage basins. The highest values of S2S3 all occur in small elongated basins between parallel ridges (many of which occur in the northwestern Sahara), but this parameter really requires a sampling region with dimensions comparable to the terrain wavelength and thus does not provide much information with this data set. Others, like ELEV_RELF (Fig. 5a) and SINUOSITY (Fig. 5d) provide information not present in any of the other parameters and their low overall correlations actually represent an advantage because they are not redundant like so many of the slope measures.

4 Discussion

Wechsler (2007) looked at uncertainties in DEMs and how they impacted hydrologic applications. She emphasized that the results of using DEMs depended on both the DEM quality, and its scale. The results reported here rely on 15″ data for drainage delineation, appropriate for global analysis, but could be extended to 3″ scale by using the full resolution of the SRTM data. The most significant problem will be the holes in the data, and lack of coverage at high northern latitudes, but the SRTM appears to be the best candidate for a global dataset for the immediate future. Initial claims for the superiority of the 1″ ASTER GDEM do not appear to be substantiated (Guth, 2010; Slater et al., 2011), and even the 1″ SRTM data currently restricted to the US military and publicly available only for the continental United States does not provide much improvement over the global 3″ data for morphometry (Guth, 2006).

Despite the limitations of scale and data quality, the SRTM drainage data provides a real bonanza for quantitative geomorphology. The challenge will be to frame the correct comparisons, which will probably involve restricting analysis to basins with similar size or Strahler order, and looking at the subbasins within the global data set. The elevation data from SRTM consists of about 35 GB of data, yet cheap processing and storage allows manipulation on common desktop computers.

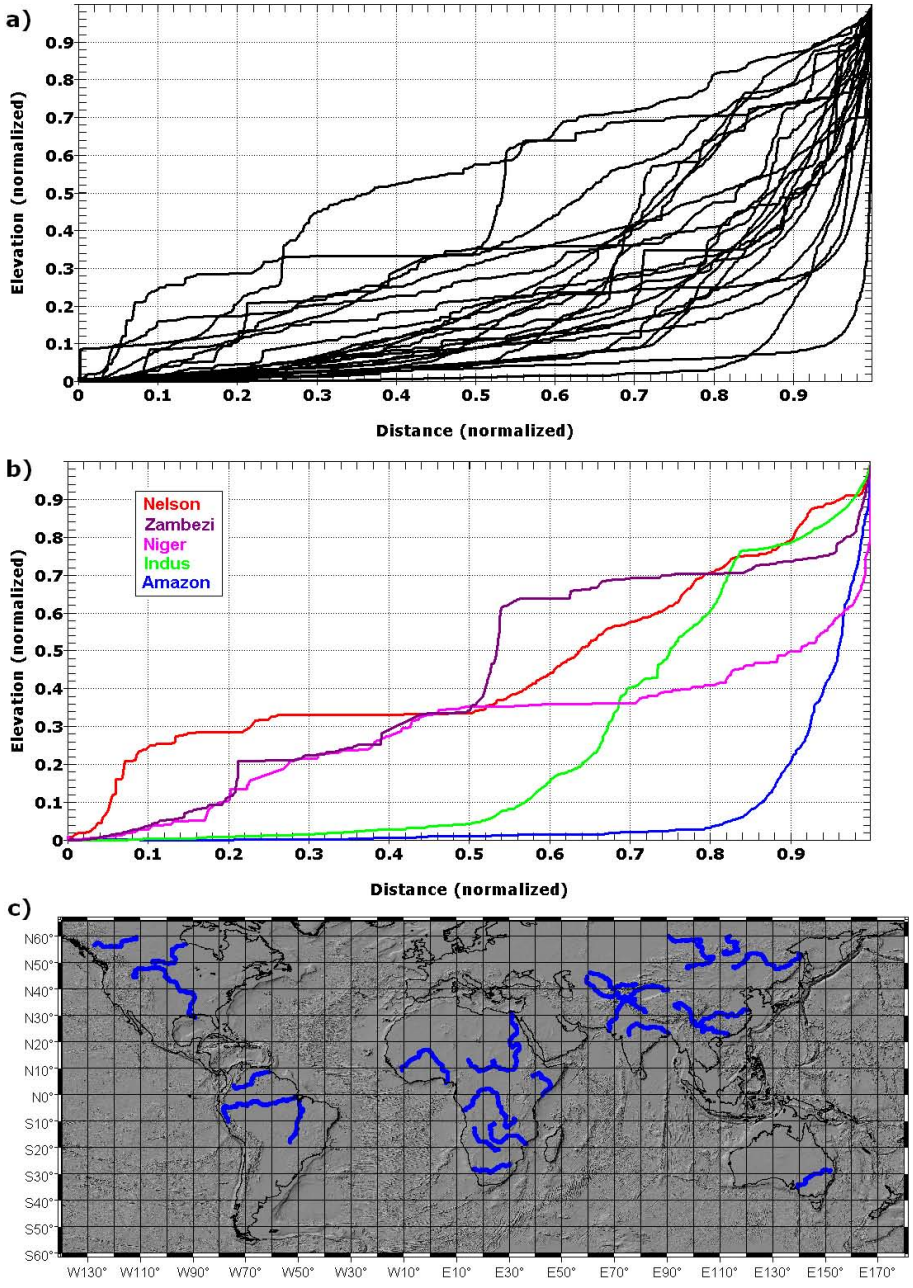

Fig. 7. Thalwegs for the 25 largest global drainage basins (thalweg relief > 500 m, Strahler order > = 8): **(a)** normalized basin profiles for all 25 thalwegs; **(b)** labeled thalwegs for 5 channels; **(c)** locations for the thalwegs depicted.

5 Conclusions

The SRTM-derived Hydrosheds data set contains 26 272 basins with an area greater than 100 km^2, and provides a near-global, internally consistent data set to investigate the gemorphological properties of both the basin and the thalweg profiles. The current resolution of this data is 15″ (about 1/2 km), appropriate for global studies. Most parameters depend on the scale of the data used for computations; classic examples include the fractal nature of coastline length, or decreasing slope values as DEM grid size increases. These results cannot be readily compared to other studies but they do permit comparisons between basins and regions within this data set. Parameters also depend on the size of the drainage basin as well as the resolution of the input data, but the SRTM data provides a fascinating picture of the world's drainage patterns.

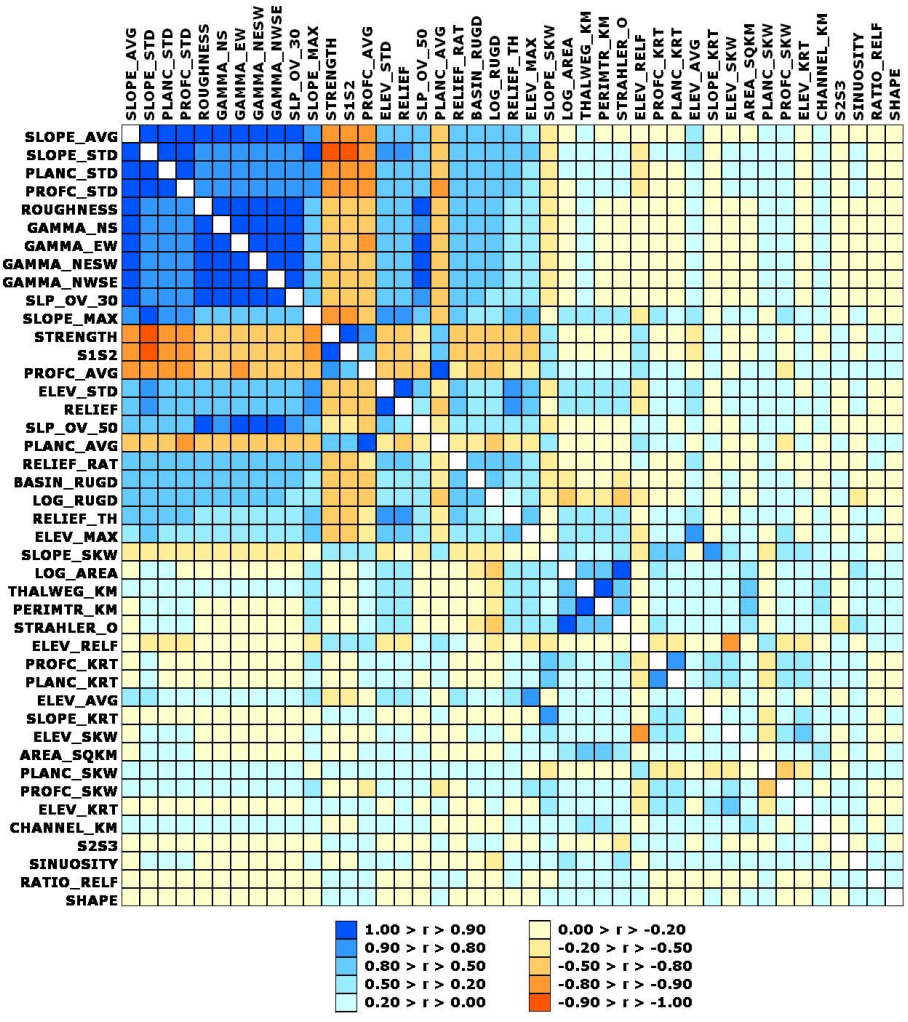

Fig. 8. Correlation matrix for the parameters in Appendix B for all drainage basins larger than 100 km^2, listed in order of parameter similarity.

Appendix A

Processing steps

1. Create a basin identifier for each basin, which combines the basin number from Hydrosheds with a two digit code for the continent, which allows linking the data sets for each basin and looking at multiple continents simultaneously.

2. Remove basins with areas less than 100 km^2 from the 15″ Hydrosheds database. This reduced the 2.48 million basins in the original data set to 26 272.

3. Create a DEM for each basin, using 6″ SRTM data created by decimating the 3″ Hydrosheds void-filled data. This size allows in-memory manipulation of the largest drainage basins for fast processing, and is still higher resolution than the drainage basins.

4. Assign each drainage segment to a basin using a point in area function; segments in the small drainage basins are left unassigned.

5. Extract nodes and create topology for each basin from the nodes at the end of each drainage segment, and compute its Strahler order

6. Create thalweg for each basin as a 3-D shapefile with elevations from the 15″ Hydrosheds DEM (6″ DEM produces similar results).

7. Compute morphometric parameters listed in Appendix B for each drainage basin.

8. Modify Hydrosheds river files to include the basin to which each river segment belongs, its Strahler order, and whether it lies on the thalweg of the drainage system.

9. Modify the Hydrosheds basin files to include Strahler order, the total length of channels in the basin, the length of the thalweg, and the perimeter of the basin.
10. Manually identify significant basins by reference to atlases and other reference material.

Appendix B

Geomorphometric parameters

1. NPTS: number of points in drainage basin (6″ DEM).
2. ELEV_AVG: average elevation (6″ DEM).
3. ELEV_STD: standard deviation of elevation (6″ DEM).
4. ELEV_SKW: skewness of elevation (6″ DEM).
5. ELEV_KRT: kurtosis of elevation (6″ DEM).
6. RELIEF: elevation range [Max$Z$–Min$Z$] (6″ DEM).
7. ELEV_MAX: maximum elevation (6″ DEM).
8. ELEV_RELF: Elevation-relief ratio or hypsometric integral or coefficient of dissection ([ELEV_AVG–Min Elevation]/RELIEF) (Pike and Wilson, 1971; Etzelmuller, 2000; Strahler, 1952).
9. SLOPE_MAX: maximum slope in percent (6″ DEM). Slope computed with Evans (1998) method, modified for DEM spacing in arc seconds.
10. SLOPE_AVG: Steepness or Roughness, average slope (6″ DEM).
11. SLOPE_STD: standard deviation of slope (6″ DEM).
12. SLOPE_SKW: skewness of slope (6″ DEM).
13. SLOPE_KRT: kurtosis of slope (6″ DEM).
14. S1S2: flatness, or slope inverse (Guth, 2003).
15. S2S3: terrain organization (Guth, 2003). High values correlate with strong tendency for ridges and valleys to align.
16. STRENGTH: alternate formulation for flatness (Fisher et al., 1987).
17. SHAPE: alternate formulation for terrain organization (Fisher et al., 1987).
18. ROUGHNESS: strong correlation with slope (Mark, 1975; Etzelmuller, 2000).
19. PROFC_AVG: average profile curvature (6″ DEM). Computed with equations in Wood (1996) based on earlier suggestions from Evans.
20. PROFC_STD: standard deviation of profile curvature (6″ DEM).
21. PROFC_SKW: skewness of profile curvature (6″ DEM).
22. PROFC_KRT: kurtosis of profile curvature (6″ DEM).
23. PLANC_AVG: average plan curvature (6″ DEM). Computed with the equations in Wood (1996) based on earlier suggestions from Evans.
24. PLANC_STD: standard deviation of plan curvature (6″ DEM).
25. PLANC_SKW: skewness of plan curvature (6″ DEM).
26. PLANC_KRT: kurtosis of plan curvature (6″ DEM).
27. GAMMA_EW: Nugget variance from the variogram (Curran, 1988), east-west direction. This measures the elevation difference from each point to its nearest neighbor; smaller values reflect smooth terrain, and high values rougher terrain (6″ DEM)
28. GAMMA_NS: Nugget variance, north-south direction.
29. GAMMA_NESW: Nugget variance, northeast-southwest direction.
30. GAMMA_NWSE: Nugget variance, northwest-southeast direction.
31. SLP_OV_30: percentage of drainage basin with slope exceeding 30 % (6″ DEM).
32. SLP_OV_50: percentage of drainage basin with slope exceeding 50 % (6″ DEM).
33. AREA_SQKM: basin area.
34. THALWEG_KM: length of the basin's thalweg.
35. CHANNEL_KM: total length of channels in drainage basin.
36. RELIEF_TH: difference in elevation (m) along the basin thalweg.
37. BASIN_RUGD: basin RELIEF (m)/AREA_SQKM
38. LOG_RUGD: log (base 10) of (basin relief/basin area)
39. RATIO_RELF: RELIEF_TH (m)/THALWEG_KM
40. STRAHLER_O: Strahler order (Strahler, 1957) computed from the 15" drainage network. Sometimes called the Strahler-Horton order.
41. PERIMTR_KM: perimeter of 15″ drainage basin.
42. SINUOSITY: ratio of main thalweg length to straight line distance connecting thalweg endpoints.

Supplementary material related to this article is available online at: http://www.hydrol-earth-syst-sci.net/15/2091/2011/hess-15-2091-2011-supplement.zip.

Acknowledgements. I thank the World Wildlife Foundation and United States Geological Survey for creating and distributing the Hydrosheds data set; obviously this analysis could not have been done without their work. I thank the three reviewers for very thoughtful and helpful comments and suggestions. Shapefiles for the river networks, drainage basin outlines and geomorphometric parameters, and 3-D basin thalwegs can be downloaded from http://www.usna.edu/Users/oceano/pguth/srtm/hydrosheds_geomorph.htm.

Edited by: S. Gruber

References

Curran, P. J.: The semivariogram in remote sensing: an introduction, Remote Sens. Environ., 24, 493–507, 1988.

Etzelmuller, B.: On the quantification of surface changes using grid-base digital elevation models (DEMs), Transact. GIS, 4, 129–143, 2000.

Evans, I. S.: What do terrain statistics really mean?, in: Landform monitoring, modelling and analysis, edited by: Lane, S. N., Richards, K. S., and Chandler, J. H., J. Wiley, Chichester, 119–138, 1998.

Farr, T. G., Rosen, P. A., Caro, E., Crippen, R., Duren, R., Hensley, S., Kobrick, M., Paller, M., Rodriguez, E., Roth, L., Seal, D., Shaffer, S., Shimada, J., Umland, J., Werner, M., Oksin, M., Burbank, D., and Alsdorf, D.: The shuttle radar topography mission, Rev. Geophys., 45, RG2004, doi:10.1029/2005RG000183, 2007.

Fisher, N. L., Lewis, T., and Embleton, B. J. J.: Statistical analysis of spherical data, Cambridge University Press, p.330, 1987.

Guth, P. L.: Terrain organization calculated from digital elevation models, in: Concepts and Modelling in Geomorphology, International Perspectives, edited by: Evans, I. S., Dikau, R., Tokunaga, E., Ohmori, H., and Hirano, M., online at http://www.terrapub.co.jp/e-library/ohmori/pdf/199.pdf, last access: 6 July 2011, Terrapub Publishers, Tokyo, 199–220, 2003.

Guth, P. L.: Geomorphometry from SRTM: Comparison to NED, Photogramm. Eng. Rem. S., 72, 269–277, 2006.

Guth, P. L.: Geomorphometry in MICRODEM, in: Geomorphometry: concepts, software, applications, Developments in Soil Science Series, edited by: Hengl, T. and Reuter, H. I., Elsevier, Amsterdam, 351–366, 2009.

Guth, P. L.: Geomorphometric comparison of ASTER GDEM and SRTM, ASPRS/CaGIS 2010 Fall Specialty Conference, Orlando, FL, 15–19 November 2010, 10 page paper on Conference CD-ROM, 2010.

Jarvis, A., Reuter, H. I., Nelson, A., and Guevara, E.: Hole-filled SRTM for the globe Version 4, available from the CGIAR-CSI SRTM 90 m Database: http://srtm.csi.cgiar.org (last access: 6 July 2011), 2008.

Lehner, B., Verdin, K., and Jarvis, J.: New global hydrography derived from spaceborne elevation data, EOS, 89, 93–94, 2008a.

Lehner, B., Verdin, K., and Jarvis, J.: HydroSHEDS Technical Documentation Version 1.1: http://gisdata.usgs.gov/webappcontent/HydroSHEDS/downloads/HydroSHEDS_TechDoc_v11.pdf (last access: 6 July 2011), 2008b.

Mark, D. M.: Geomorphometric parameters: A review and evaluation, Geogr. Ann. A, 57, 165–177, 1975.

Pike, R. J. and Wilson, S. E.: Elevation-relief ratio, hypsometric integral and geomorphic area-altitude analysis, Geol. Soc. Am. Bull., 82, 1079–1084, 1971.

Pike, R. J., Evans, I. S., and Hengl, T.: Geomorphometry: A brief guidd, in: Geomorphometry: concepts, software, applications, Developments in Soil Science Series, edited by: Hengl, T. and Reuter, H. I., Elsevier, 1–30, 2009.

Simley, J. D. and Carswell Jr., W. J.: The National Map – Hydrography: U.S. Geological Survey Fact Sheet, 2009–3054, http://pubs.usgs.gov/fs/2009/3054/ (last access: 6 July 2011), p.4, 2009.

Slater, J. A., Heady, B., Kroenung, G., Curtis, W., Haase, J., Hoegemann, D., Shockley, C., and Tracy, K.: Global assessment of the new ASTER Global Digital Elevation Model, Photogramm. Eng. Rem. S., 77, 335–349, 2011.

Strahler, A. N.: Hypsometric (area-altitude) analysis of erosional topography, Geol. Soc. Am. Bull., 63, 1117–1142, 1952.

Strahler, A. N.: Quantitative analysis of watershed geomorphology, Trans. Am. Geophys. Un., 8, 913–920, 1957.

Wechsler, S. P.: Uncertainties associated with digital elevation models for hydrologic applications: a review, Hydrol. Earth Syst. Sci., 11, 1481–1500, doi:10.5194/hess-11-1481-2007, 2007.

Wood, J. D.: The geomorphological characterisation of digital elevation models, http://www.soi.city.ac.uk/~jwo/phd/, last access: 6 July 2011, unpublished PhD Thesis, University of Leicester, UK, 1996.